



Investigating the role of solvent extraction in altering pH levels for efficient Neodymium extraction from magnet scrap



Huwaiddah I. Ahmed ^{a,b*} , Ali A. Aljubouri ^a, Hanaa A. AL-Kaisy ^c 

^a College of Applied Science, University of Technology-Iraq, Alsina'a street, 10066 Baghdad, Iraq.

^b College of Production Engineering and Metallurgy, University of Technology-Iraq, Alsina'a street, 10066 Baghdad, Iraq.

^c College of Materials Engineering, University of Technology-Iraq, Alsina'a street, 10066 Baghdad, Iraq.

*Corresponding author Email: as.21.26@grad.uotechnology.edu.iq

HIGHLIGHTS

- At pH ≤ 2 , the concentration of rare earth elements and metal ions increased, enhancing the extraction potential.
- D2EHPA acted as an efficient cation exchanger, releasing H⁺ ions during metal cation uptake.
- In solvent extraction, precipitated particles promoted rare earth attachment to extractant compounds.
- The highest neodymium extraction efficiency was achieved at a pH of 1.5.
- The addition of neodymium to magnesium improved its corrosion resistance.

Keywords:

Rare earth
Neodymium
Magnet
Solvent extraction
Corrosion

ABSTRACT

Recycling rare earth elements, specifically neodymium from magnet scrap, is crucial for advancing sustainable technologies across various industries. In this research, neodymium was recovered by solvent extraction using a stock solution prepared in 200 mL by dissolving 1 g of neodymium (III) nitrate hexahydrate, Nd(NO₃)₃.6H₂O, in 0.5 M nitric acid. Then, it was mixed with 1 M di-(2-ethylhexyl) phosphoric acid (D2EHPA) in Isopar-L, as the organic phase, and 3 M H₂SO₄, as the aqueous phase, with an organic/aqueous volume ratio of (1:1). Specifically, the study examined the pH variation of the aqueous phase (from 0.5 to 2). The pH of the solution was measured using a pen-type pH meter, where the stripping agent was HNO₃ at a concentration of 6 M. The experiments were conducted using a magnetic stirrer at ambient temperature with an agitation speed of 300 rpm for 24 hours. The concentration of metals was measured using an EDX. The extraction efficiency of neodymium increased from 51.7% at a pH of 0.5 to 82.02% at a pH of 1.5, with a slight decrease observed at pH values of 1.7 and 2. Moreover, samples of Mg-Nd alloy were manufactured with various extractant Nd contents of (1, 3, 4, and 5%). The microstructure of the alloys, both before and after corrosion in 3.5% NaCl, was examined using a scanning electron microscope (SEM). The results indicated that the alloys consisted primarily of the α -Mg phase and the Mg₁₂Nd phase, and that the corrosion resistance increased with the increasing amount of neodymium.

1. Introduction

One of the world's most significant problems with recycling neodymium from magnets is that refining rare earth elements (REEs), such as neodymium, comes with significant environmental burdens. It may also produce greenhouse gas emissions, lead to water contamination, and cause habitat destruction. Furthermore, neodymium supply is based on a handful of countries, leading to political risks and foreseeable shortages of the metal. Additionally, the recycling of neodymium from magnets nearing the end of their life is technically and logically challenging [1].

However, recycling neodymium from magnets saves both the environment and money. In addition, this recycling process decreases the demand for new mining, is less environmentally hazardous, and is more energy-efficient compared to the production process of neodymium from its ores. Moreover, recycling generates value from what is now considered electronic waste, contributing to a more sustainable and circular economy. In this context, NdFeB magnet scraps have been widely investigated and recycled in different ways. Among these techniques for recycling REEs from Nd-Fe-B magnet waste, the hydrometallurgical processes listed in Table 1 seem more promising because they can be used for any magnet. These processes must, first and foremost, be closely tied to the existing REE production industry [2]. In this regard, NdFeB magnets are currently recycled hydrometallurgically by leaching the magnet material with an acid to dissolve the rare earth elements and then precipitating neodymium as a salt or an oxide. According to this process, neodymium can be selectively precipitated from the

solution as a compound, such as neodymium oxalate, or as a mixed rare earth precipitate by controlling the pH value and using a precipitating agent, such as oxalic acid. The secondary technique is solvent extraction, which can also be used to extract neodymium from the other cations in solution using suitable organic solvents. The other type of method is ion exchange, and other purification processes can be used to purify the Nd [3]. To this end, solvent extraction is frequently used in the hydrometallurgical sector to extract metals from minerals, ores, or metal scrap. In particular, the pH value of the solution is a crucial parameter in the extraction process. Optimal separation occurs at a modified pH value, particularly in the case of neodymium extraction using various organic extractants [4,5].

Nowadays, academic researchers pay more attention to the leaching of magnet scrap. For instance, Reisdörfer et al. [6], reported that the dissolution of neodymium was readily achieved using malic acid by leaching NdFeB powder in a solvent extraction process. Particularly, they found that 360 minutes of filtrate treatment, a process of treating the liquid that has passed through a filter, with unroasted NdFeB powder, achieved 100% neodymium recovery. However, a drawback of this work is that it was limited to unroasted NdFeB powder and a single filtration time. NI'AM et al. [7], conducted a study in 2020 about the extraction of neodymium from waste permanent magnets through leaching and solvent extraction using D2EHPA in Isopar-L. However, other potential solvents or extractants were not empirically investigated in the study, nor was the influence of different process parameters, such as temperature, pH, or stripping conditions, which restricts the applicability of the results to other leaching and solvent extraction. Moreover, Prusty et al. [8], studied ionic liquids as an emerging alternative for the separation and recovery of Nd, Sm, and Eu using a solvent extraction technique with quaternary ammonium. The researchers concluded that ionic liquids are a promising alternative for separating rare earth elements; however, they suffered from several limitations, including high viscosity, potential degradation of fluorinated anions, and higher cost compared to conventional extractants.

In another study, Allahkarami et al. [9], investigated the extraction of neodymium (III) from aqueous solutions with Cyanex® 572 extractant. The findings showed that non-polar diluents were suitable for extracting neodymium (III). However, CYANEX 572 cannot be used for the general separation and extraction of REEs. In particular, it exhibits a lower extraction capacity for LREEs. In addition, Rizk et al. [10], detailed that the less polar phase Cyanex 572 in kerosene successfully extracts Gd (III) and Nd(III) in the presence of LiNO₃ when mixed with the polar phase (ethylene glycol). Nevertheless, the primary disadvantage of using Cyanex 572 in kerosene for solvent extraction is its inability to separate some REEs adequately, especially in mixed solutions. Furthermore, Villoutreys [11], investigated the solvent extraction method for the separation of Nd (III) from a specific acidic leach liquor of monazite. The primary shortcoming of this approach, however, is that it utilized data for a specific type of leach liquor and selected REEs (Ce, La, Nd, Pr).

In this context, Bashiri et al. [12], summarized the central potential mechanisms for REE separation by membranes, including complexation within the membrane or adsorption on active sites, as well as rejection of REE ions. However, the intricate matrices, as well as diverse conditions common in real REE sources, were not fully accounted for in the study. In another work, Srivastava et al. [13], investigated solvent extraction (SE) for the separation of REEs using the Di(2-ethylhexyl) phosphoric acid (DEHPA)/TBP extractant. Nevertheless, the limitation is that Nd, Pr, and Ce are difficult to separate successfully by this model due to their similar chemical properties. Zhang et al. [14], investigated the corrosion performance of the binary alloys Mg-7%Nd and Mg-10%Y. The researchers concluded that the corrosion rates of two alloys are mainly influenced by the micro-galvanic corrosion between the second phase and the α -Mg matrix. In addition, Belfqueh et al. [15], studied the selective recovery of rare earth elements from the acetic leachate of NdFeB magnets using solvent extraction. The researchers concluded that TODGA enables the selective extraction of rare earths; however, this method faces challenges in achieving a complete separation of individual REEs from one another.

Based on what mentioned above, this study aims to investigate the optimal pH value for the most efficient extraction of neodymium from the scrap of decommissioned NdFeB magnets and to highlight the importance of neodymium in the corrosion prevention of Mg-Nd binary alloys.

Table 1: A comparison of various rare earth element separation technologies applicable to NdFeB permanent magnet waste [16]

Methods	Advantages	Disadvantages
Precipitation	The process is simple with low cost	It is difficult to obtain a single REE, and the low recovery product is impure.
Solvent extraction	Can obtain high-purity single rare earth	The process involves complex procedures and generates substantial quantities of waste, accompanied by increased expenses.
Ionic liquids extraction	Can obtain high-purity single rare earth efficiently	The difficulty in preparing an ionic liquid system and the high cost associated with it.

2. Materials and methods

2.1 Materials

In this investigation, neodymium magnets were obtained by gathering several discarded hard disk drives, disassembling them, and extracting the magnets. Chemical acids (37% HCl), neodymium nitrate hexahydrate (Nd(NO₃)₃.6H₂O, 99.9%), and di-2-ethylhexyl phosphoric acid (D2EHPA, 98% molecular weight of 322.42 g/mol) as an acidic extractant in Isopar-L were purchased from Macklin Company (China), and distilled water was used.

2.2 Testing instrumentation

In this work, the following devices were utilized; The NQM-0.4 Model planetary ball mill (Yangzhou Nuoya Machinery Co., Ltd.) from China, the particle size analyzer nano brook (90 Plus), Brookhaven Instruments, which is a company based in the United States, the Manual Hydraulic Press (Han14468) made in China, Potentiostat/Galvanostat Corr test (model CS350M) from China, and the MTI, Tube Furnace GSL 1600X from the Lab World Group in the USA. All the above devices are available at the University of Technology's Nanotechnology Advanced Materials Research Centre in Baghdad, Iraq. The Axia Chemi SEM is a product of Thermo Fisher Scientific, a global company based in the United States. The XRD is a product of Malvern PANalytical, a spectroscopy company (UK), located in Al-Khora Laboratories, Iraq-Baghdad. In addition, a magnetic stirrer device (obtained from Joan Lab, HSSS AC220V, China) was used, along with various-sized flasks, a separating funnel, and a pen-type pH meter (PH-009 (I) from China.

2.3 Experimental procedure

2.3.1 Pretreatment

A set of inoperable hard disks was acquired, and the exterior covers and screws were removed. The disk contains a neodymium magnet. The demagnetization procedure was conducted at 300, 350, 400, and 450 °C for 15 and 30 minutes, respectively. Due to their thinness and fragility, the magnets are readily broken. After being crushed and ground into tiny particles for 60 minutes in a planetary ball mill, the composition was analyzed. In more detail, the amount of metal content in the magnets was determined using energy-dispersive X-ray spectroscopy (EDX).

2.4 Leaching studies

The leaching experiments were conducted in closed Erlenmeyer flasks. Typically, 200 mL was used with a magnetic stirrer device. A 3M H₂SO₄ solution was added to the Erlenmeyer flasks. Then, the magnet scrap powder was added to the acid solution with a solid-to-liquid (S/L) ratio of 0.3. The leaching time was held constant at 24 hours to ensure maximum leaching of metals. In this regard, the minimum agitation speed of the magnetic stirrer required to keep all particles in suspension is 300 rpm, which is applied during the leaching step at room temperature.

2.4.1 Solvent extraction studies

A stock solution of 1g. Nd(NO₃)₃.6H₂O in 0.5 M nitric acid was mixed with 1M D2EHPA in Isopar-L as the organic phase, and 3M H₂SO₄ as the aqueous phase with a 1:1 A/O ratio. The study includes varying the pH values of the aqueous phase (from 0.5 to 2). In practice, we can adjust the pH of the aqueous phase by using acid HCl to decrease the pH value or by using base NaOH to increase the pH value. The stirring of the two-phase system was conducted at ambient temperature with a 300-rpm agitation speed over 24 hours using a magnetic stirrer. Then, the two phases should be separated using a separation funnel. Next, the separated organic solution, loaded with REE, was mixed with 6M HNO₃ to strip it back into the aqueous phase. The REE ratio was verified using energy-dispersive X-ray spectroscopy (EDX).

2.4.2 Magnesium-neodymium alloy preparation

Magnesium powder was obtained from the Maclean Company and re-ground using a planetary ball mill to achieve a fine aggregate particle size. Specifically, the extractant Nd powder was added in different proportions of (1, 3, 4, and 5%). The pressing was done using a pressing mould with a 1 cm diameter and a 4 cm height. More precisely, the mould was placed under eight tons of pressure in a hydraulic press. After removing the samples, the sintering process was performed using a vacuum electric furnace. Subsequently, the compressed samples with varying percentages of the element neodymium were placed in small alumina crucibles, and the annealing process was conducted at a temperature of 500 °C, followed by cooling within the furnace.

2.4.3 Corrosion studies

The Potentiostat/Galvanostat Corr test model CS350M was used for corrosion testing. In this regard, a 3.5% sodium chloride saline solution was prepared and placed in the designated place within the apparatus. One-centimeter-diameter and one-centimeter-high cylindrical samples were immersed in the solution for 15 minutes, and the corrosion current and the corrosion rate were calculated using the same device.

3. Results and discussion

3.1 Magnet characterization

In this study, EDX was used to examine the waste from milled demagnetized permanent magnets. In particular, Table 2 indicates that the demagnetized samples are primarily composed of the elements Fe and neodymium, with trace amounts of boron, dysprosium, and praseodymium. The FE-SEM image in Figure 1 indicates the presence of heterogeneous and irregularly shaped particles [17].

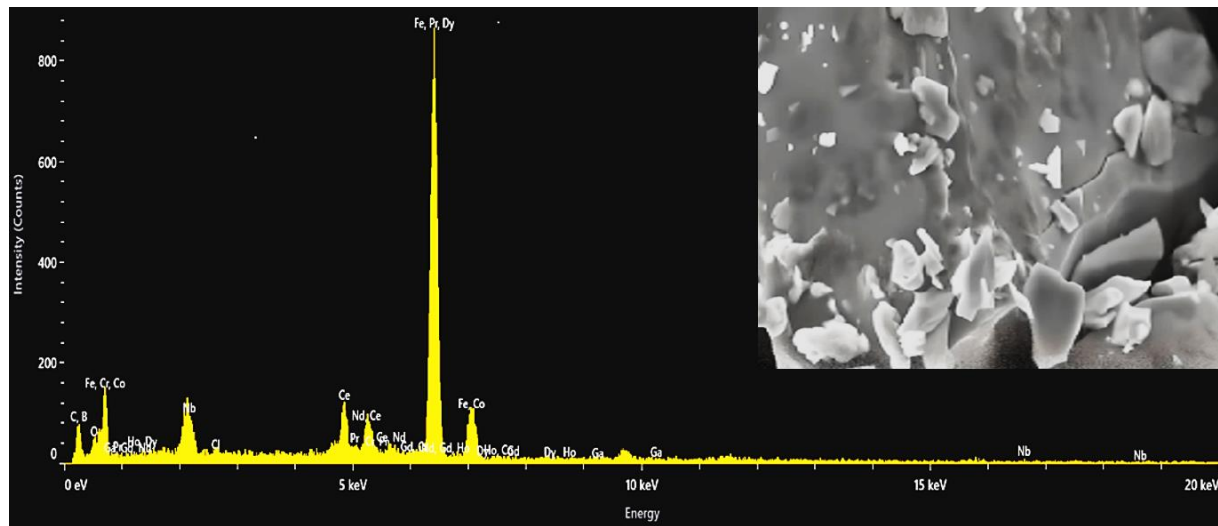


Figure 1: The FE-SEM image and the EDX analysis of the magnet powder

Table 2: Chemical composition of NdFeB magnet waste (EDX analysis)

Element	B	Cr	Fe	Co	Ga	Nb	Ce	Pr	Nd	Gd	Dy	Ho	Ni	Zr
Weight %	1.7	0.1	62.1	0.1	0.2	1.0	1.3	2.2	29	0.05	1	0.6	2.0	0.95

3.2 The X-ray Diffraction (XRD) Analysis for Magnet Scrap

The X-ray diffraction (XRD) pattern of the NdFeB magnet, as shown in Figure 2, predominantly indicates the presence of the $\text{Nd}_2\text{Fe}_{14}\text{B}$ tetragonal phase, which is the principal magnetic phase responsible for the material's profound magnetic properties. In particular, the peaks observed in the pattern are characterized by their sharpness and intensity, signifying a well-defined crystalline structure and a high degree of purity in the magnetic phase. The peak positions, represented by the 2θ values, along with their relative intensities, can be systematically compared with established JCPDS data (specifically JCPDS 00-036-1296) to validate both the existence and the quality of this phase [18,19]. The pattern sometimes reveals peaks that correspond to other minor phases, including the Nd-rich phases (for instance, Nd or Nd_2O_3) [20].

The existence of these phases can affect both magnetic properties and microstructure, and their presence may vary depending on the specific magnet and its processing methods. To determine Miller indices from XRD data, it is essential to identify the diffraction peaks, calculate the d-spacings using Bragg's Law, and subsequently correlate these d-spacings with Miller indices by utilizing the crystal structure and lattice parameters.

In certain instances, the XRD pattern may reveal the texture, or preferential orientation, of the grains, particularly in the context of sintered or hot-deformed magnets. Any discrepancies observed in the anticipated peak intensities may signify complications related to grain orientation and can serve as a basis for refining processing parameters. Moreover, the breadth of the XRD peaks can provide insights into the grain size and the crystallinity of the various phases present. Peak broadening may result from the presence of smaller grain sizes, lattice strain, or other microstructural imperfections. Additionally, peak intensities are influenced by the relative proportions of each phase, as well as their respective crystallographic textures [21,22].

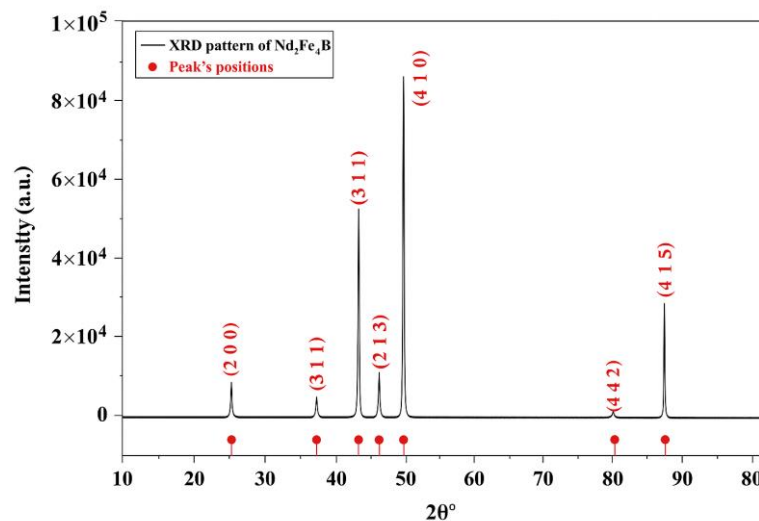


Figure 2: The XRD pattern for the magnet scrap

3.3 Particle size analysis

The particle size of the used neodymium magnet powder measured by a particle size analyzer was equal to 64.4 nm, as shown in Figure 3. In this regard, the dimensions of the magnetic particles considerably influence the efficacy of the extraction processes. Typically, reduced particle sizes contribute to enhanced extraction rates owing to an expanded surface area available for chemical reactions and accelerated diffusion rates [23]. Conversely, larger particle sizes may be associated with lower extraction rates and increased oxygen content [24].

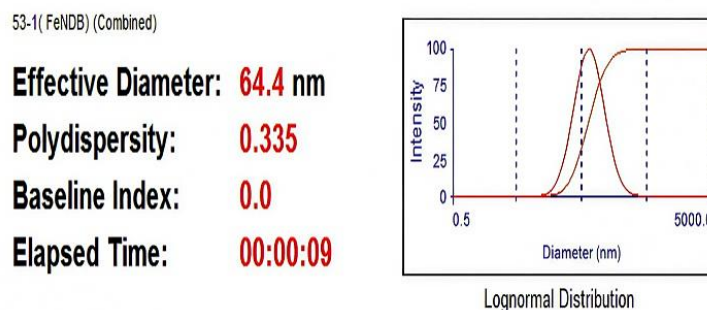


Figure 3: The particle size of the neodymium magnet scrap

3.4 The extractant agent used in the solvent extraction

In the separation of neodymium (Nd), various extractants are used in the solvent extraction series, as shown in Table 3. Specifically, the extractor systems for the separation of rare earths include acidic organophosphorus extractants, such as di-2-ethylhexyl phosphoric acid (D2EHPA) and PC88A, as well as neutral extractants like Cyanex 923 and trioctylphosphine oxide (TOPO). Moreover, ionic liquids, such as trihexyl(tetradecyl)phosphonium thiocyanate, are also used in conjunction with the neutral extractants [25].

In this context, the D2EHPA (Di-2-ethylhexylphosphoric acid) is commonly used for the solvent extraction of REEs. It can also include rare earth ions, for which the selective extraction from aqueous solutions can be transferred to an organic phase. To this end, REEs can be efficiently separated from chloride media using D2EHPA, and high levels of the elements are obtained in the organic phase during the extraction process. In particular, the D2EHPA is a chelating agent that creates highly stable complexes with rare-earth metal ions. The MaC/DTPA complexes are then stripped from the aqueous phase to the organic phase (typically diluted in Isopar L), with the latter containing REEs (the extraction phase) separated from the former [26].

It was concluded that, in terms of cost, solubility, future supply availability, and ease of extracting neodymium, the D2EHPA is the most likely solvent for neodymium extraction. Here, neodymium was preferentially extracted to a large extent from the leachate, while other elements, such as iron, manganese, and cobalt, mainly remained in the aqueous phase. In addition, the organic neodymium extractant can be easily stripped by the dilute nitric acid (6 M HNO₃), and the D2EHPA does not dissolve. Therefore, although many divalent and trivalent metal ions exist in the leachate, neodymium can be effectively extracted through the D2EHPA method, and the D2EHPA extractant exhibits good stability and reusability [27].

Table 3: Various extraction systems are utilized for the separation of rare earth elements

Rare earth	Extractant	Diluent	Aqueous Medium	Water-soluble-Complexing Agent	Remarks
Lanthanum, Praseodymium, and Neodymium	Cyanex 272 PC88A	Escaid 110	Chloride	EDTA	The inclusion of EDTA in the aqueous phase is believed to facilitate the extraction of bromine and neodymium by the formation of anionic complexes. PC88A exhibits superior extraction efficiency compared to Cyanex 272.
Lanthanum, cerium, praseodymium, and neodymium	P204	kerosene	Chloride	Lactic acid, citric acid	The separation factors for cerium-lanthanum (Ce/La) and praseodymium-lanthanum (Pr/La) were enhanced in the system that incorporated both complexing agents.
Neodymium/praseodymium	D2EHPA	kerosene	Chloride	Lactic acid	The enhancement of the distribution ratio and the separation factor is attributed to a decrease in acidity alongside an increase in lactic acid concentration, which resulted in the optimal separation factor for neodymium and praseodymium.

3.4.1 Challenges in solvent extraction

Solvent extraction of neodymium from NdFeB magnets presents several challenges, primarily in separating neodymium from iron and other materials in the magnet alloy. These challenges include issues with leaching selectivity, the need to ensure high purity while avoiding the co-extraction of unwanted elements like iron, and the necessity of managing the environmental impact of solvents. Particularly, many solvents used in solvent extraction are toxic or hazardous, requiring careful handling and disposal. In such cases, emulsions can form, making it difficult to separate the two liquid phases. Moreover, volatile and flammable solvents pose significant safety risks, necessitating the implementation of additional measures to mitigate these hazards. In addition, high-purity solvents can be expensive, thereby increasing the overall cost of the process [28].

Furthermore, the process can be labour-intensive, time-consuming, and may require large amounts of solvent [29]. In this respect, the separation of REEs using D2EHPA as an extractant has been widely studied due to its relatively high separating factor for RE batch tests. However, its limited solubility hinders further application for large-scale separation. In particular, the concentrated D2EHPA in mixed solvents has been successfully applied to separate REEs on a semi-industrial scale. However, forming the third phase during the solvent extraction operation is an inevitable challenge that must be overcome. The third phase formation is closely associated with the concentrations of D2EHPA and REEs during the extraction and back-extraction operation. Orders of magnitude higher concentrations of D2EHPA were reported to afford high extraction performance. However, at such high D2EHPA concentrations, a standard alkane diluent cannot provide a clear extracting phase, thereby hindering the further application of D2EHPA as a cost-efficient solvent extraction reagent. Other mixed diluents were also tested with up to 10% D2EHPA. All these mixed diluents, however, could not afford the high extraction capacity and the separation factor of the standard alkane diluent [29].

3.4.2 Significance of pH in neodymium extraction

At pH levels ≤ 2 , the concentration of rare earth elements increases in the aqueous phase, and the amount of metal ions increases, providing a greater extraction potential. As shown in Figure 4, the extraction efficiency increased from 51.7% at a pH value of 0.5 to 82.02% at a pH value of 1.5, with a slight decrease at pH values of 1.7 and 2 [30].

Neodymium may be present as a soluble neodymium ion in aqueous solution. In an environment with a pH value of 2 or less, the rare earth elements, such as neodymium, significantly increased in the aqueous phase. This increase causes a larger quantity of metal ions to be generated, resulting in improved extraction capability. Keep in mind that when dissolved in water, neodymium exists as an ion that can be soluble. However, at a pH value of 2 or lower, neodymium forms a positively charged ion that can bind freely in the solution and is neutralized electromagnetically. This means that thymol cannot exist without forming a covalent bond at a high pH value. Ionization occurring here is imperative for successful extraction, as the goal is to separate neodymium from the rest of the composition and make it accessible in liquid form. Consequently, these findings demonstrate the value of alternative neodymium recovery in acidic environments. In this regard, maintaining a pH value of 2 or lower within a high-concentration electrolyte ensures that the majority of the neodymium is ionized, thereby maximizing the extraction efficiency [31, 32], which can be calculated using Equation 1 [33].

$$\text{Extraction Efficiency (\%)} = \frac{\text{Actual Amount Extracted}}{\text{Theoretical Maximum Amount}} \times 100 \quad (1)$$

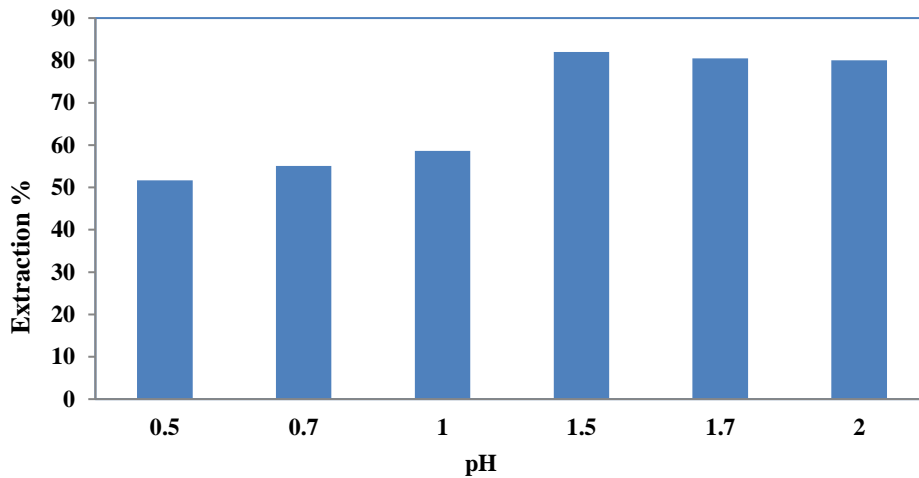


Figure 4: Effect of pH values of the solution on effectiveness of neodymium extraction

3.4.3 The EDX spectrum analysis

The EDX (Energy Dispersive X-ray) is a powerful technique used to analyze the elemental composition of materials, including REEs. It works by detecting X-rays emitted from a sample when bombarded with an electron beam, with the energy of these X-rays being characteristic of the elements present. In the context of rare earths, the EDX can be used to identify and quantify the presence of elements such as dysprosium, praseodymium, neodymium, and others in various materials, as shown in Figure 5 (a-f). The EDX technique was used to examine rare earth elements and iron in the organic phase loaded with rare earth at different pH levels. Specifically, the peak intensity corresponds to the element's relative abundance in the sample, such as neodymium.

The primary factor influencing peak intensity is the abundance of the rare earth element within the analyzed material. Specifically, a higher concentration means that more atoms are available to emit X-rays when excited, resulting in a stronger signal and a higher peak. Each element emits X-rays with characteristic energies, and these energies are used to identify the element [34,35].

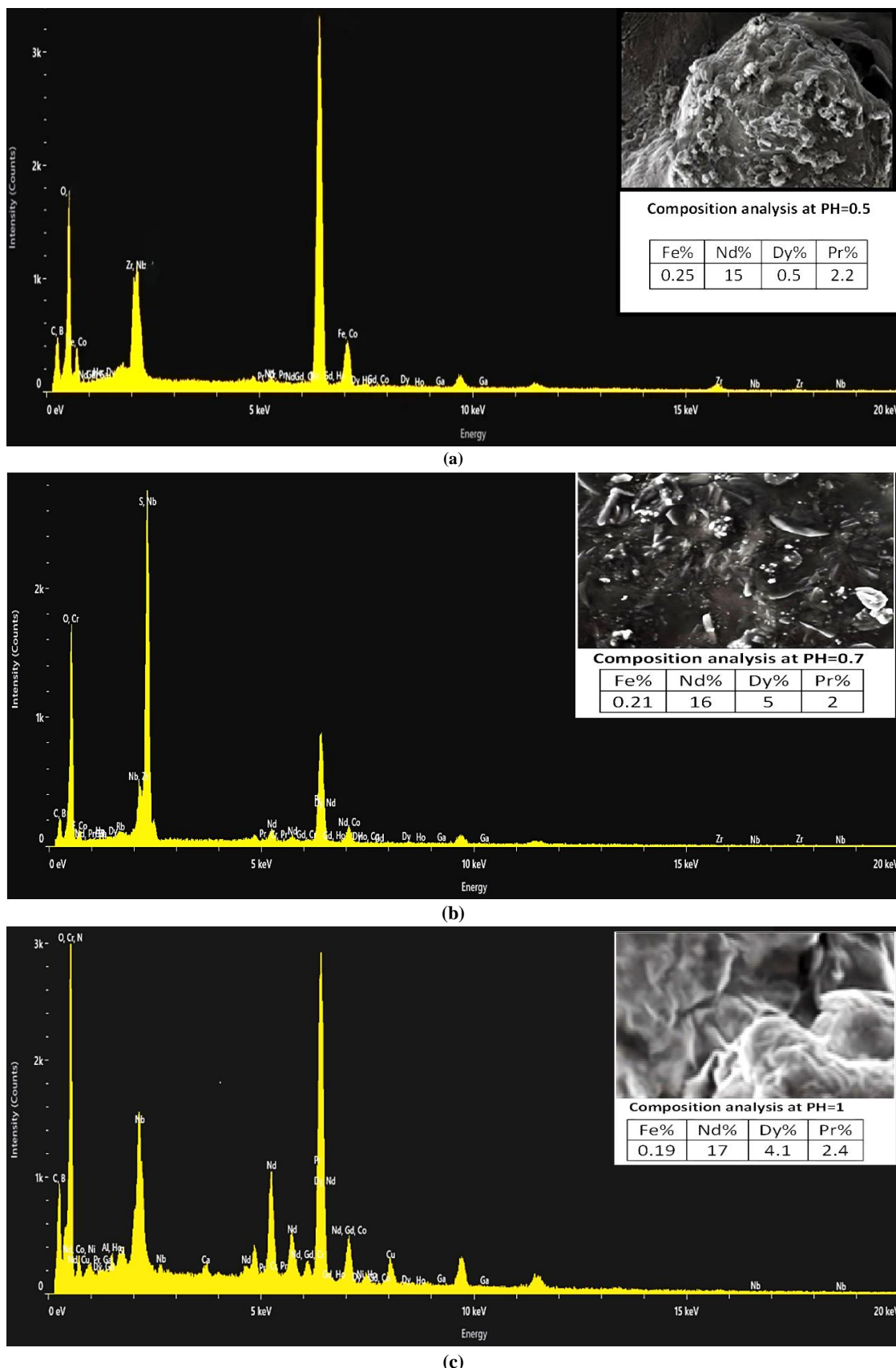


Figure 5: (a-f) The FE-SEM image and the EDX analysis of samples at different pH values

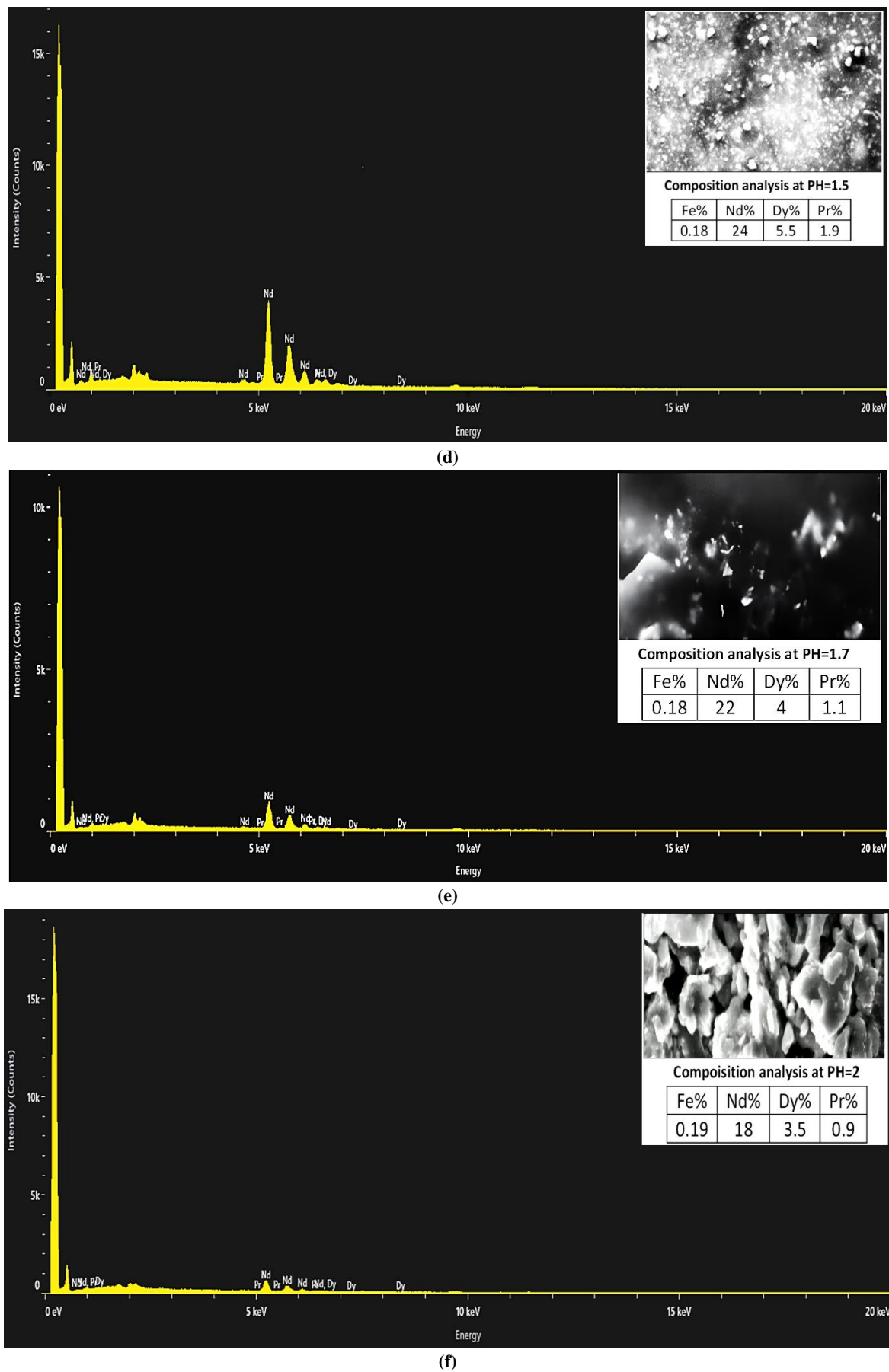


Figure 5: Continued

3.4.4 The stripping process

Following solvent extraction, the REEs can be stripped back into the aqueous phase using an organic phase loaded with rare earth elements from the previous step. Accordingly, a 6 M nitric acid solution was used as the stripping agent. The acidic solution breaks the bond between the REEs and the chelating agent, causing the REEs to transfer into the aqueous phase. The organic solvent, now free of REEs, can be recycled back into the extraction process. To this end, minimizing the amount of aqueous waste generated during stripping is an important consideration [36]. Subsequently, the aqueous solution containing the stripped REEs can then be further processed. This stage may involve additional purification steps, such as the precipitation of individual REEs using specific reagents, such as sodium carbonate [37].

In practice, precipitation is typically carried out by adding a solution of sodium carbonate (Na_2CO_3) to an aqueous solution containing the REEs, leading to the formation of insoluble neodymium carbonate ($\text{Nd}_2(\text{CO}_3)_3$), which precipitates out of the solution as a solid.

When a base like sodium hydroxide (NaOH) is added to a solution containing dissolved neodymium (III) carbonate ($\text{Nd}_2(\text{CO}_3)_3$), the pH value increases, causing the hydroxide ions (OH^-) from the base to react with the neodymium ions (Nd^{3+}), this reaction forms neodymium(III) hydroxide ($\text{Nd}(\text{OH})_3$), which is a less soluble precipitate [38]. Next, neodymium hydroxide ($\text{Nd}(\text{OH})_3$) is converted to neodymium oxide (Nd_2O_3) via calcination, which involves heating to 550 °C. This oxide is then reduced to neodymium metal [39,40].

After completing the above process, an EDX test was performed on the sample extracted at a pH value of 1.5, and the results are shown in Figure 6. We notice the presence of a small percentage of copper metal. Particularly, copper appears after neodymium extraction from NdFeB magnets due to the presence of copper in the protective coating of the magnets, which dissolves into the leaching solution along with neodymium during the extraction process. Specifically, when these magnets are leached with sulfuric acid, copper from the coating dissolves, leading to its presence in the resulting solution alongside neodymium [41].

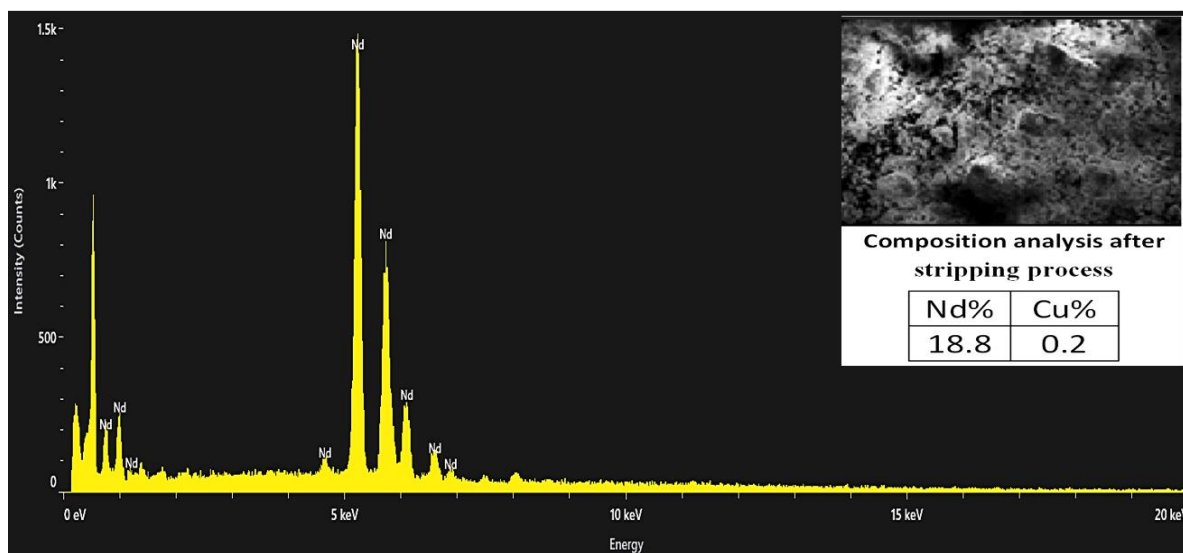


Figure 6: The FE-SEM image and the EDX analysis of the extractant material after the stripping and purification steps

3.4.5 Waste disposal after extraction of neodymium from magnets

Aqueous waste is often treated through neutralization by adding a base (such as lime) to neutralize the acid, forming a precipitate, and precipitation by separating dissolved metals through the process of precipitating them out as hydroxides or other salts. In contrast, organic waste is often treated through solvent recovery, where distillation or other techniques are used to recover and reuse the solvent. Additionally, incineration or specialized disposal may be employed, requiring contaminated solvents to be incinerated or disposed of at specialized facilities [42].

4. Neodymium as an alloying element

Neodymium has been regarded as a valuable candidate to improve the performance of magnesium alloys. Due to its large electropositivity and low solubility, the addition of Nd can create an extensive metal-neodymium phase in magnesium alloys, which enhances their strength and ductility. In this regard, competition is intensifying in the exploitation of materials and resources. In particular, there is a growing need to minimize material consumption to the lowest possible level. One development direction is to develop their highly economical alloys, like the neodymium-containing alloy, as a new type of magnesium alloy material. However, there are limited research results on the corrosion of magnesium-rare earth alloys compared to the extensive study of other magnesium alloy systems. According to the results, as the amount of Nd increased, the shape of the second phase changed from islands or bands to a network structure. Specifically, all second phases are made up of the Mg_{12}Nd phase [43,44].

4.1 Phase Transformations in Mg-Nd Alloy

Phase transformations in Mg-Nd alloys begin with the formation of a second phase, which is a solid solution of Nd in Mg [45]. To study the isothermal part of the phase diagram, samples of Mg-x at.% Nd ($x=1,3,4,5$) are considered when sintered in a

vacuum furnace. A solid solution of Nd is combined with another solid solution containing Mg to form the nanostructures. For the studied range of Nd concentrations, the structure of the solid solution of Nd in Mg is linked to the changes in the starting state throughout the phase transition. According to the SEM images shown in Figure 7 (a-d), the structure was normal dendritic, composed of a grid with α -Mg phase grey areas and a second phase represented by Mg12Nd white areas. If more Nd were added to the Mg, the second phase would move around in different ways. It was primarily observed at the grain boundary of the Mg-1%Nd alloy, where it exhibited a dotted pattern. Moreover, it was spread out along the grain boundaries of the Mg-3%Nd alloy and had a short, rod-like shape. In the Mg-4%Nd alloy, a second-phase network structure was created [46].

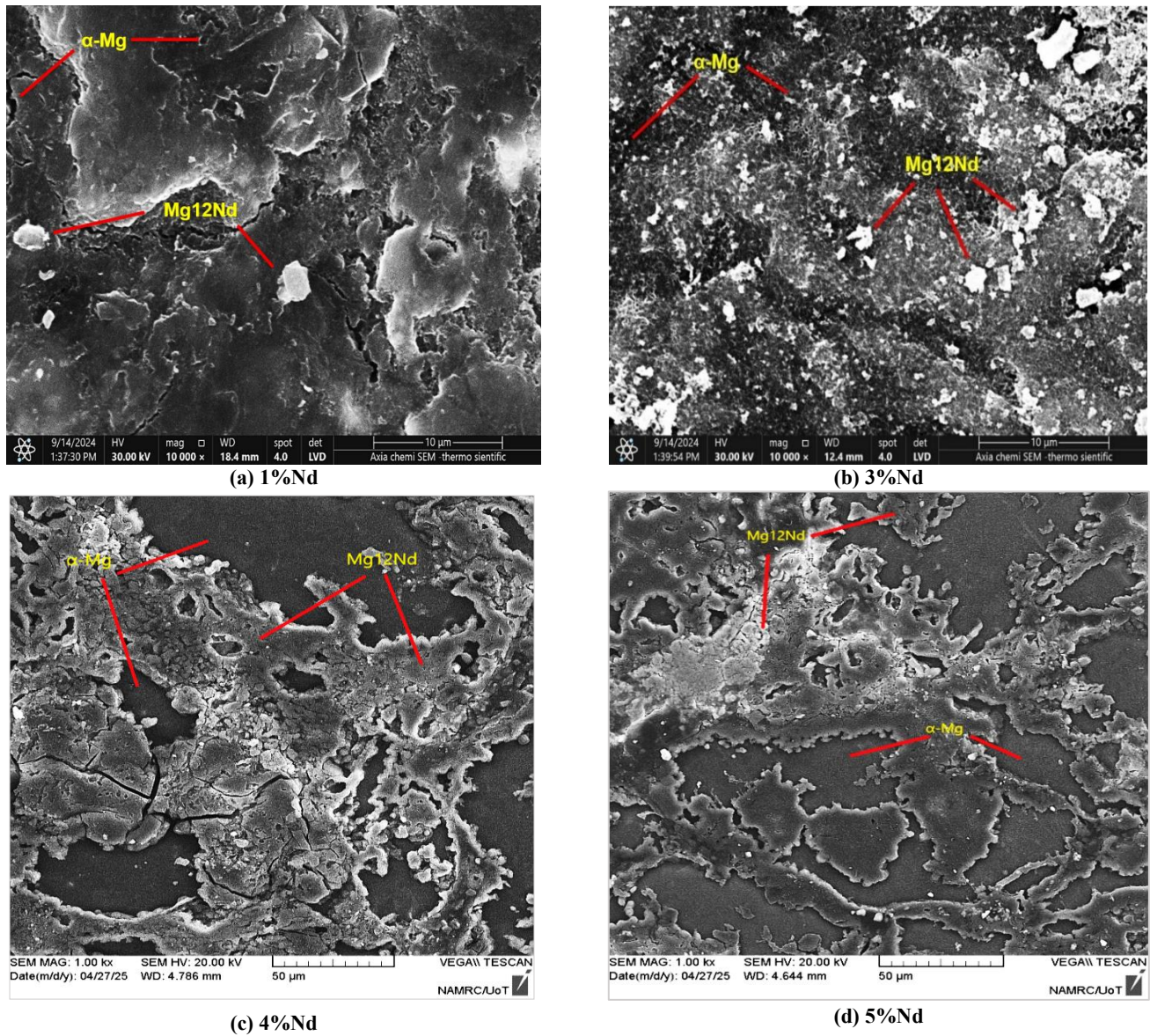


Figure 7: (a-d) The microstructure of the Mg-Nd alloys using SEM

4.2 Corrosion behaviour of the magnesium-neodymium alloys

The corrosion current in 3.5% saline solution decreases as the percentage of the Nd element increases, with the lowest corrosion rate observed at 5% Nd, as shown in Figure 8, due to the influence of the network phase on the corrosion resistance of the Mg-Nd alloys.

Particularly, the microstructure consisted of nearly continuous networks of the β phase that penetrated the compositionally pure α phase. The effect of Nd introduced in industrially produced Mg-Nd binary alloys on the microstructure and corrosion properties in saline solutions is reported to result in a high content of the β phase during the corrosion process, as shown in Figure 9 (a-d). The breakdown of the microstructure, which leads to corrosion in the Mg-Nd areas between grains, is linked to the amount of Nd, the size of the grains, and the amount of the second phase. These factors are also linked to a decrease in the concentration of the second phase within the pores. Increasing the amount of neodymium (Nd) can increase corrosion resistance by forming a more continuous and stable passive film (like Nd_2O_3) on the alloy surface, which acts as a barrier against corrosive agents. This protective film suppresses the electrochemical dissolution of the alloy matrix, resulting in reduced corrosion rates and enhanced corrosion resistance [47].

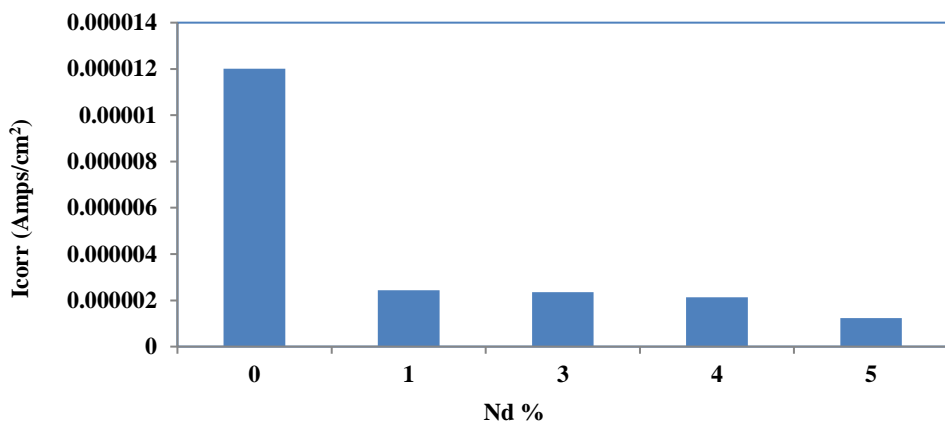


Figure 8: The relationship between the corrosion current (Icorr) and the Nd content

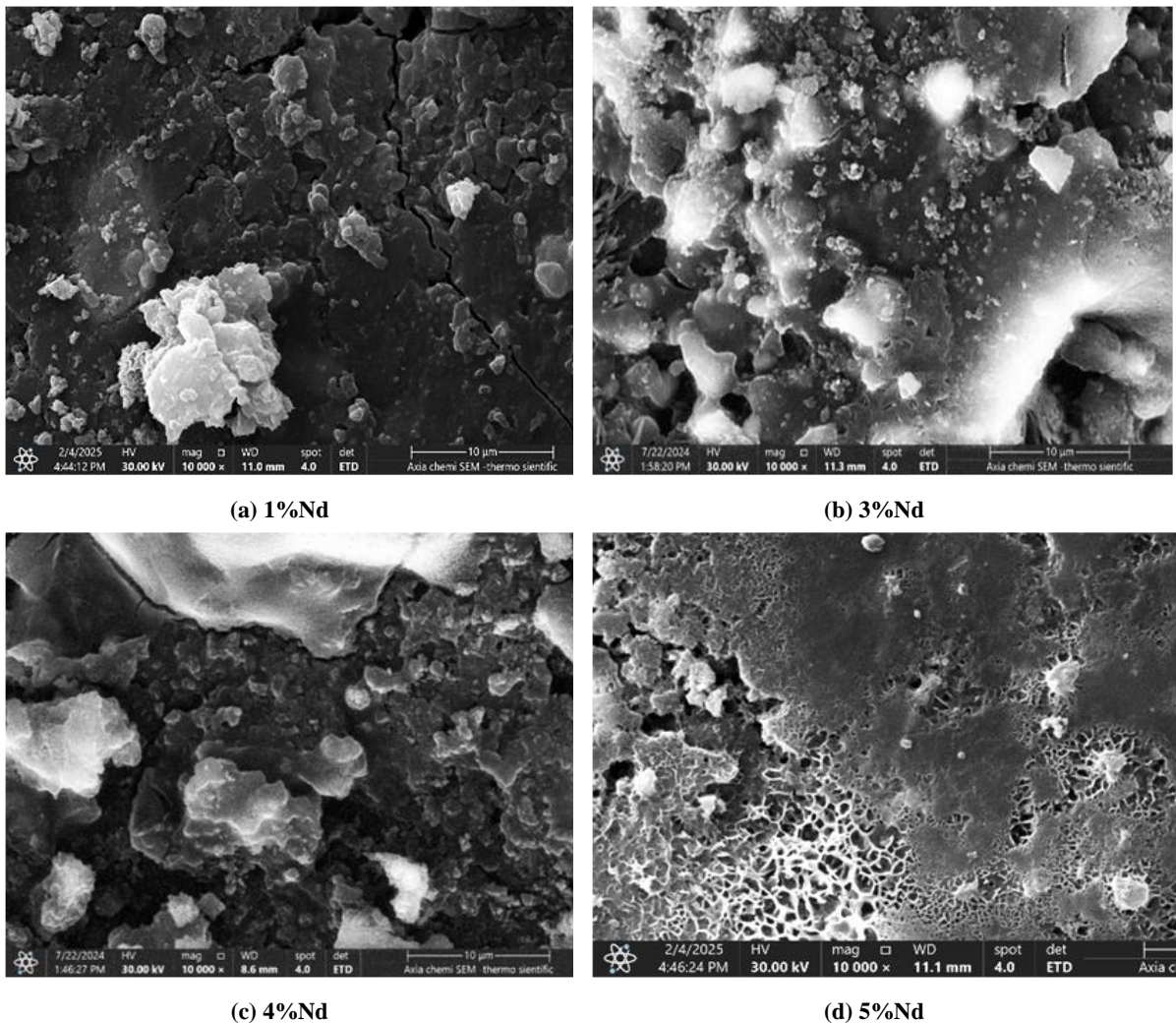


Figure 9: (a-d) The microstructure of the Mg-Nd alloys after immersion in a 3.5% salt solution using SEM

4.2.1 Polarization resistance of the Mg-Nd Alloy

The polarization resistance, R_p , of an electrode is defined explicitly as the slope of the potential (E) versus the current density (I_{corr}) around the corrosion potential (E_{corr}). This crucial parameter is essential for gaining insights into the electrode's electrochemical behaviour and the overall performance. It indicates the resistance that the electrode surface exhibits to current flow when it is slightly perturbed from its equilibrium state, which is vital for evaluating the corrosion rates and predicting the long-term stability of materials in various environments. The values of R_p were calculated utilizing Equation 2 [48].

$$R_p = \frac{ba bc}{2.303(ba+bc)I_{corr}} \quad (2)$$

In practice, understanding R_p enables the design and utilization of electrodes in practical applications [49]. In this regard, magnesium and neodymium have relatively close standard electrode potentials [47].

The results of the measured Polarization Resistance (R_p) of the Mg-Nd alloy samples tested at a Potentiostat/Galvanostat Corr in a 3.5% NaCl environment are presented in Table 4. It is possible to correlate some observed differences in the polarization resistance of the samples with their alloy composition. Specifically, samples with the lowest concentration of alloying elements demonstrate the lowest corrosion resistance. On the other hand, samples with the highest nominal alloying element concentration exhibit the highest corrosion resistance, as indicated by the R_p value in Figure 10 (a-e) and the absence of a corrosive region. In the active state, the electrode responds to changes in potential slowly until the limit of the Tafel region is reached. In contrast, in the corrosive state, the electrode reactions are fast, which accounts for a precipitous increase in the final current. The derivative curve is read from cathodic to anodic parts, rather than the conventional direction, anodic to cathodic parts; however, numerous overlapping variables may alter the electrochemical responses. Some variable exemplars include alloy composition, temperature, and environmental conditions [50].

In the analysis development, a Tafel method was employed, which involved conducting the potentiodynamic polarization process as a one-variable experiment. In this respect, the polarization curve behaviour may change depending on a material's microstructure. Moreover, there may be independent microstructural variables that directly affect the performance of the Nd-containing Mg alloys. Overall, the polarization curves must be conducted to test the material performance in a specific application, as they do not always suffice in conjunction with other experimental observations [51].

Table 4: Corrosion parameters for the Mg-Nd alloys with different neodymium contents

Nd%	ba (mv)	bc (mv)	Icorr (Amps/cm ²)	Corrosion rate (mm/a)	Ecorr (volts)	R _P (Ω.cm ² *10 ³)
0	43.987	30.531	12.006E-06	0.14084	-0.86285	0.651
1	40.477	25.233	2.4367E-06	0.028585	-1.2703	2.769
3	49.064	33.373	2.3488E-06	0.02201	-1.29482	3.671
4	43.987	30.531	2.1325E-06	0.02001	-1.4151	3.669
5	67.078	85.549	1.2308E-06	0.014439	-1.485	13.264

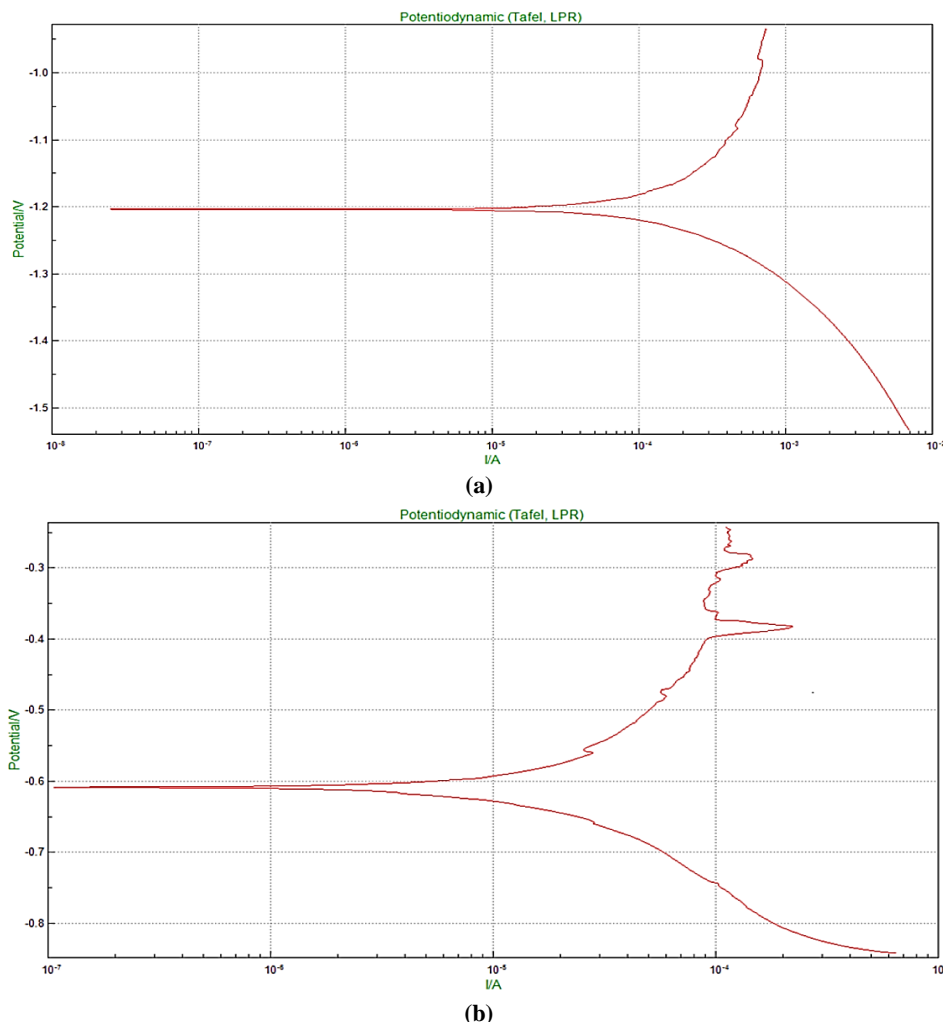


Figure 10: The polarization curve for the Mg-Nd alloy with different neodymium contents a) pure Mg, b) 1% c) 3% d) 4%, and e) 5%

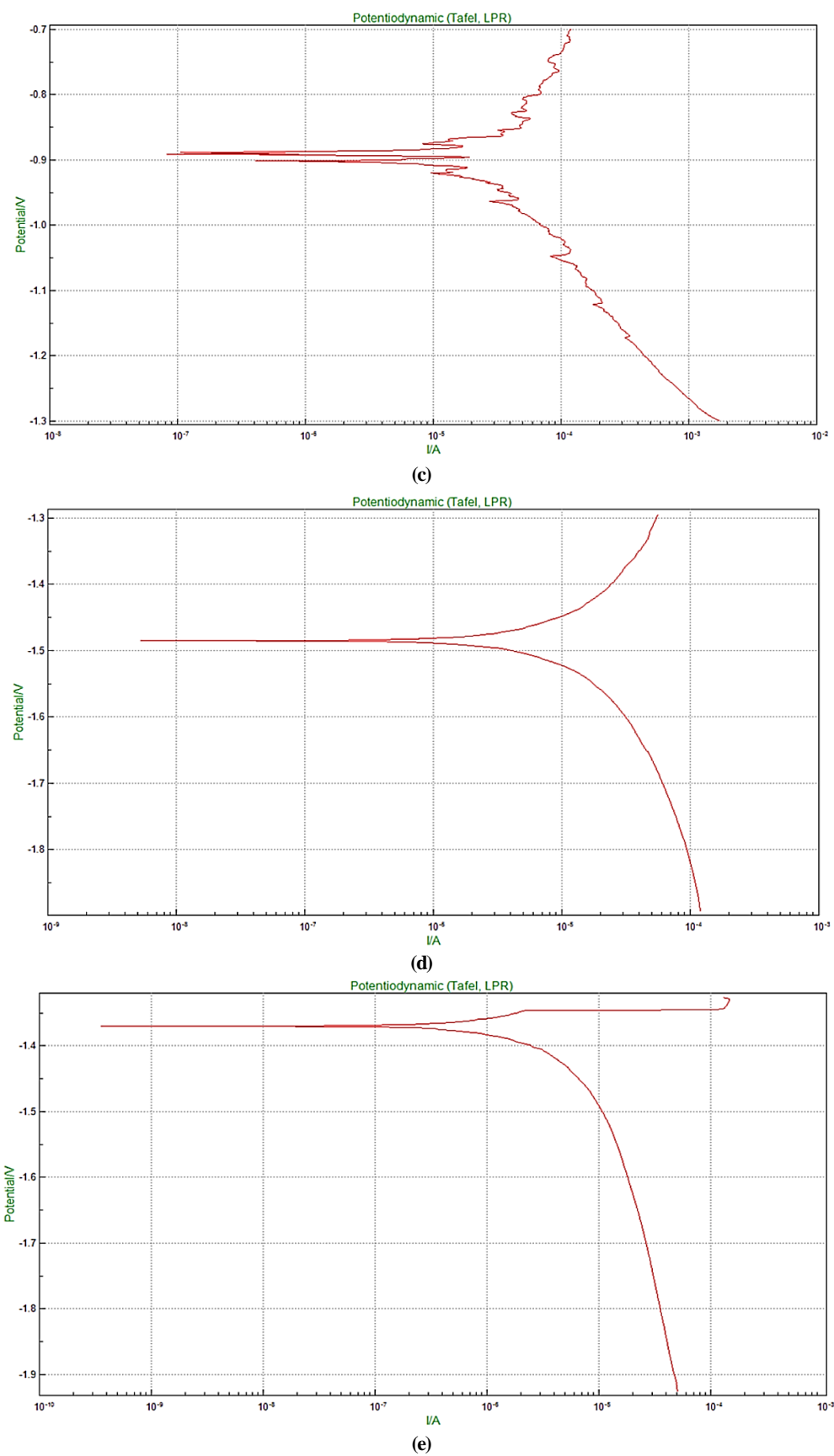


Figure 10: Continued

5. Conclusion

The most important conclusions from this study are as follows:

- 1) D2EHPA forms complexes with rare earth ions, allowing for their separation from aqueous solutions by transferring them into an organic phase.
- 2) D2EHPA is particularly effective in separating REEs from chloride media, with high extraction rates reported for the rare earth elements.
- 3) D2EHPA acts as a chelating agent, forming strong complexes with rare earth ions of metal. After that, these complexes are transferred from the aqueous phase into an organic phase, usually diluted with isopar L. The organic phase, containing the extracted REEs, can then be separated from the aqueous phase.
- 4) At pH levels ≤ 2 , neodymium forms a positively charged ion that can bind freely in the solution. In this regard, maintaining a pH level of ≤ 2 within a high-concentration electrolyte ensures that the majority of the neodymium is ionized, which maximizes extraction efficiency.
- 5) At pH levels ≤ 2 , the concentration of rare earth elements increases in the aqueous phase, and the amount of metal ions increases, providing a greater extraction potential. More specifically, the extraction efficiency increased from 51.7% at a pH value of 0.5 to 82.02% at a pH value of 1.5, with a slight decrease at pH values of 1.7 and 2.
- 6) The stripping agents (HNO_3) and their concentration (6 M) are the best for stripping rare earth elements. Subsequent chemical processes are effective in extracting the neodymium.
- 7) The microstructure of the Mg-Nd alloy is composed of separated eutectic Mg_{12}Nd and dendritic α -Mg. An interphase network becomes apparent at 4% neodymium addition, and the volume fraction of the interphases rises as neodymium addition increases.
- 8) The experimental results showed that with the increase of the Nd content from 1 to 5%, the corrosion resistance of the Mg-Nd alloy in the physiological saline environment is enhanced.

Author contributions

Conceptualization, **H. Ahmed, A. Aljubouri** and **H. AL-Kaisy**; data curation, **H. Ahmed**; formal analysis, **H. Ahmed**; investigation, **H. Ahmed**; methodology, **H. Ahmed**; project administration, **A. Aljubouri**; resources, **H. AL-Kaisy**; software, **H. Ahmed**; supervision, **A. Aljubouri** and **H. AL-Kaisy**; validation, **A. Aljubouri**, and **H. AL-Kaisy**; visualization, **A. Aljubouri** and **H. AL-Kaisy**; writing—original draft preparation, **H. Ahmed**; writing—review and editing **A. Aljubouri**, and **H. AL-Kaisy**. All authors have read and agreed to the published version of the manuscript.

Funding

This research received no specific grant from any funding agency in the public, commercial, or not-for-profit sectors.

Data availability statement

The data that support the findings of this study are available on request from the corresponding author.

Conflicts of interest

The authors declare that there is no conflict of interest.

References

- [1] C. Burkhardt, S. Van Nielen, M. Awais, F. Bartolozzi, J. Blomgren, P. Ortiz, M. B. Xicotencatl, An overview of Hydrogen-assisted (Direct) recycling of Rare earth permanent magnets, *J. Magn. Magn. Mater.*, 588 (2023) 171475. <https://doi.org/10.1016/j.jmmm.2023.171475>
- [2] M. Kaya, An overview of NdFeB magnets recycling technologies, *Curr. Opin. Green Sustain. Chem.*, 46 (2024) 100884. <https://doi.org/10.1016/j.cogsc.2024.100884>
- [3] P. Romano, S. Rahmati, R. Adavodi, G. Clementini, F. Gallo, F. Veglio, Study of the kinetics and mechanisms of rare earth elements leaching from end-of-life NdFeB magnets through Hydro-Nd process, *Sep. Purif. Technol.*, 356 (2025) 129850. <https://doi.org/10.1016/j.seppur.2024.129850>
- [4] M. I. Martín, I. García-Díaz, F. A. López, Properties and perspective of using deep eutectic solvents for hydrometallurgy metal recovery, *Miner. Eng.*, 203 (2023) 108306. <https://doi.org/10.1016/j.mineng.2023.108306>
- [5] P. Romano, S. Rahmati, R. Adavodi, G. Clementini, F. Gallo, F. Veglio, Study of the kinetics and mechanisms of rare earth elements leaching from end-of-life NdFeB magnets through Hydro-Nd process, *Sep. Purif. Technol.*, 356 (2025) 129850. <https://doi.org/10.1016/j.seppur.2024.129850>
- [6] G. Reisdörfer, D. Bertuol, E. H. Tanabe, daniel bertuolb, Eduardo Hiromitsu Tanabe, recovery of neodymium from the magnets of hard disk drives using organic acids, *Miner. Eng.*, 143 (2019) 105938. <https://doi.org/10.1016/j.mineng.2019.105938>

[7] A. C. NI'AM, Y. H. Liu, Y. F. Wang, S. W. Chen, G. M Chang, S. J. You, Recovery of Neodymium from Waste Permanent Magnets by Hydrometallurgy Using Hollow Fibre Supported Liquid Membranes, *Solvent Extr. Res. Dev. Jpn.*, 27 (2020) 69-80. <https://doi.org/10.15261/serdj.27.69>

[8] S. Prusty, S. Pradhan, S. Mishra, Ionic liquid as an emerging alternative for the separation and recovery of Nd, Sm and Eu using solvent extraction technique-A review, *Sustain. Chem. Pharm.*, 21 (2021) 100434. <https://doi.org/10.1016/j.scp.2021.100434>

[9] E. Allahkarami, B. Rezai, M. Bozorgmehr, S. Adib, Extraction of neodymium (III) from aqueous solutions by solvent extraction with Cyanex® 572, *Probl. Miner. Proces.*, 57 (2021) 127-135. <https://doi.org/10.37190/ppmp/136080>

[10] S. E. Rizk, R. Gamal, N. E. El-Hefny, Insights into non-aqueous solvent extraction of gadolinium and neodymium from ethylene glycol solution using Cyanex 572, *Sep. Purif. Technol.*, 275 (2021) 119160. <https://doi.org/10.1016/j.seppur.2021.119160>

[11] Villoutreys, É. De. Thermodynamic study of the (Ce-Nd)-Fe-B system for new permanent magnets. Ph.D. Thesis, Material chemistry, Sorbonne Université, 2024. <https://theses.hal.science/tel-04982279v1>

[12] A. Bashiri, A. Nikzad, R. Maleki, M. Asadnia, A. Razmjou, Rare earth elements recovery using selective membranes via extraction and rejection, *Membranes*, 12 (2022) 80. <https://doi.org/10.3390/membranes12010080>

[13] V. Srivastava, J. Werner, R. Honaker, Design of multi-stage solvent extraction process for separation of rare earth elements, *Mining*, 3 (2023) 552-578. <https://doi.org/10.3390/mining3030031>

[14] H. Zhang, Y. Zhao, J. Liu, J. Xu, D. Guo, C. Li, Impact of rare earth elements on micro-galvanic corrosion in magnesium alloys: A comparative study of Mg-Nd and Mg-Y binary alloys, *Int. J. Electrochem. Sci.*, 18 (2023) 100160. <http://dx.doi.org/10.1016/j.ijoes.2023.100160>

[15] S. Belfqueh, S. Chapron, F. Giusti, S. Pellet-Rostaing, A. Seron, N. Menad, G. Arrachart, Selective recovery of rare earth elements from acetic leachate of NdFeB magnet by solvent extraction, *Sep. Purif. Technol.*, 339 (2024) 126701. <https://doi.org/10.1016/j.seppur.2024.126701>

[16] Y. Zhang, F. Gu, Z. Su, S. Liu, C. Anderson, T. Jiang, Hydrometallurgical Recovery of Rare Earth Elements from NdFeB Permanent Magnet Scrap: A Review, *Metals*, 10 (2020) 841. <https://doi.org/10.3390/met10060841>

[17] L. Wang, X. Xu, Facile Synthesis of Nd₂Fe₁₄B Hard Magnetic Particles with Microwave-Assisted Hydrothermal Method, *Molecules*, 28 (2023) 7918. <https://doi.org/10.3390/molecules28237918>

[18] Y. Mehrifar, H. Moqtaderi, F. Golbabaei, S. M. Hamidi, M. Hasanzadeh, S. F. Dehghan, Characterisation of electro-spun nanofibers containing Nd₂Fe₁₄B ferromagnetic alloy nanoparticles: A promising potential for the synthesis of new magnetic, *J. Alloys Compd.*, 1007 (2024) 176301. <https://doi.org/10.1016/j.jallcom.2024.176301>

[19] L. Wang, X. Xu, Facile Synthesis of Nd₂Fe₁₄B Hard Magnetic Particles with Microwave-Assisted Hydrothermal Method, *Molecules*, 28 (2023) 7918. <https://doi.org/10.3390/molecules28237918>

[20] L. G. D Santos, D. D. A. Buelvas, D. F. Valezi, B. L. S. Vicentin, Microstructural and magnetic properties of polyamide-based recycled composites with iron oxide nanoparticles, *Magnetism*, 5 (2025) 5. <https://doi.org/10.3390/magnetism5010005>

[21] H. Chen, W. Liu, Z. Guo, T. Yang, H. Wu, Y. Qin, Y. Li, Coercivity enhancement of Nd-La-Ce-Fe-B sintered magnets: Synergistic effects of grain boundary regulation and chemical heterogeneity, *Acta Materialia*, 235 (2022) 118102. <https://doi.org/10.1016/j.actamat.2022.118102>

[22] A. Gholizadeh, V. Banihashemi, Effects of Ca-Gd co-substitution on the structural, magnetic, and dielectric properties of M-type strontium hexaferrite, *J. Am. Ceram. Soc.*, 106 (2023) 5351-5363. <https://doi.org/10.1111/jace.19191>

[23] S. A. Ajeel, F. A. Sameer, N. I. AbdulLatif, Separation of Aluminium Chloride from White Kaolinite by Slime Leaching Process, *Eng. Technol. J.*, 32 (2014) 2412-0758. <https://doi.org/10.30684/etj.32.7A8>

[24] D. Talan, Q. Huang, A review of environmental aspects of rare earth element extraction processes and solution purification techniques, *Miner. Eng.*, 179 (2022) 107430. <https://doi.org/10.1016/j.mineng.2022.107430>

[25] M. De Luccas Dourado and D. G. de Carvalho, Modeling and simulation of samarium and neodymium separation by a solvent extraction process, *Braz. J. Chem. Eng.*, 42 (2025) 413-420. <https://doi.org/10.21203/rs.3.rs-3006822/v1>

[26] R. Rodríguez Varela, A. Chagnes, K. Forsberg, Third-Phase Formation in Rare Earth Element Extraction with D2EHPA: Key Factors and Impact on Liquid Membrane Extraction Performance, *Membranes*, 15 (2025) 188. <https://doi.org/10.3390/membranes15070188>

[27] S. Laguel, M. H. Samar, Elimination of rare earth (neodymium (III)) from water by emulsion liquid membrane process using D2EHPA as a carrier in kerosene, *Desalin. Water Treat.*, 317 (2024) 100214. <https://doi.org/10.1016/j.dwt.2024.100214>

[28] S. Belfqueh, S. Chapron, F. Giusti, Selective recovery of rare earth elements from acetic leachate of NdFeB magnet by solvent extraction, *Sep. Purif. Technol.*, 339 (2024) 126701. <https://doi.org/10.1016/j.seppur.2024.126701>

[29] A. Merroune, J. Ait Brahim, B. Achiou, R. Boulif, Behaviours of rare earth elements from industrial wet-process phosphoric acid using di-(2-ethyl-hexyl) phosphoric acid solvent: optimisation and thermodynamic studies, *J. Mol. Liq.*, 367 (2022) 120585 <https://doi.org/10.1016/j.molliq.2022.120585>

[30] B. Mwewa, M. Tadie, S. Ndlovu, G. S. Simate, Recovery of rare earth elements from acid mine drainage: A review of the extraction methods, *J. Environ. Chem. Eng.*, 10 (2022) 107704. <https://doi.org/10.1016/j.jece.2022.107704>

[31] Z. Zhang, J. Liu, T. Li, Z. Fu, J. Mao, X. Li, S. Ren, Highly efficient and selective separation of dysprosium and neodymium from polyethene glycol 200 solution by non-aqueous solvent extraction with P350, *J. Mol. Liq.*, 380 (2023) 121765. <https://doi.org/10.1016/j.molliq.2023.121765>

[32] M. E. Reece, A. A. Migdisov, A. E. Williams-Jones, A. C. Strzelecki, L. Waters, H. Boukhalfa, X. Guo, Stability of aqueous neodymium complexes in carbonate-bearing solutions from 100-600 °C, *Commun. Earth Environ.*, 6 (2025) 353. <https://doi.org/10.1038/s43247-025-02334-w>

[33] L. Alcaraz , O. Rodríguez-Largo, Recovery of Rare Earths from End-of-Life NdFeB Permanent Magnets from Wind Turbines, *Chem. Sus. Chem.*, 18 (2025) e202402237. <https://doi.org/10.1002/cssc.202402237>

[34] D. A. Gkika, M. Chalaris, G. Z. Kyzas, Review of methods for obtaining rare earth elements from recycling and their impact on the environment and human health, *Processes*, 12 (2024) 1235. <https://doi.org/10.3390/pr12061235>

[35] L. Zhang, W. Xiao, G. Li, D. Wang, J. Wu, H. Du, A cleaner and sustainable method for recovering rare earth and cobalt from NdFeB leaching residues, *J. Clean. Prod.*, 422 (2023) 138576. <https://doi.org/10.1016/j.jclepro.2023.138576>

[36] A. Fayyaz, R. Ali, M. Waqas, U. Liaqat, R. Ahmad, Analysis of rare earth ores using laser-induced breakdown spectroscopy and laser ablation time-of-flight mass spectrometry, *Minerals*, 13 (2023) 787. <https://doi.org/10.3390/min13060787>

[37] A. Amidi, S. A. M. Razif, N. A. Jabit, K. S. Ariffin, Characterisation of rare earth elements (REE) from industrial REE waste resources, *Mater. Today Proc.*, 66 (2022) 3140-3143. <https://doi.org/10.1016/j.matpr.2022.07.464>

[38] Y. Yang, X. Zhang, K. Li, L. Wang, F. Niu, D. Liu, Y. Meng. Maintenance of the Metastable State and Induced Precipitation of Dissolved Neodymium (III) in an Na₂CO₃ Solution, *Minerals*, 11 (2021) 952. <https://doi.org/10.3390/min11090952>

[39] A. Phuruangrat, S. Thongtem, T. Thongtem, Template-free synthesis of neodymium hydroxide nanorods by microwave-assisted hydrothermal process and of neodymium oxide nanorods by thermal decomposition, *Ceram. Int.*, 38 (2012) 4075-4079. <https://doi.org/10.1016/j.ceramint.2012.01.065>

[40] Guo, X. Dissolution and Electrochemical Reduction of Rare Earth Oxides in Fluoride Electrolytes. Ph.D. Thesis, Delft University of Technology, 2021. <https://doi.org/10.4233/uuid:79a1f6f1-52d1-48a9-a0df-03c1b1ce0ac6>

[41] A. A. Galhoun, B. T. Mohamed, S. S. Abdulmoteleb, Solvent extraction of titanium (IV) from orthophosphoric acid media using Aliquat-336/kerosene and stripping with nitric acid, *Hydrometallurgy*, 231 (2025) 106403. <https://doi.org/10.1016/j.hydromet.2024.106403>

[42] A. Lee, A. Naquash, M. Lee, Y. D. Chaniago, H. Lim, Exploitation of distillation for energy-efficient and cost-effective environmentally benign process of waste solvents recovery from semiconductor industry, *Sci. Total. Environ.*, 841 (2022) 156743. <https://doi.org/10.1016/j.scitotenv.2022.156743>

[43] X. Xiang, Y. Wu, Z. Chen, Y. Pan, Y. Ge, Y. Zhang, Neodymium-modified Mg-Zn-Zr magnesium alloy as a biodegradable osteogenic implant, *iScience*, 28 (2025) 112677. <https://doi.org/10.1016/j.isci.2025.112677>

[44] X. Wei, S. Gao, Q. Le, L. Ren, J. Hu, J. Wu, and T. Wang, Preparation of Mg-Nd alloys by in situ reduction using Nd₂O₃, *J. Alloys Compd.*, 1004 (2024) 175720 <https://doi.org/10.1016/j.jallcom.2024.175720>

[45] X. Yan, B. Su, X. Yang, Q. Xu, X. Zhang, J. Wang, Z. Wen, Experimental and simulation investigation of Nd additions on as-cast microstructure and precipitate development in Mg–Nd system alloys, *Materials*, 15 (2022) 2535. <https://doi.org/10.3390/ma15072535>

[46] J. Wang, Y. Yuan, T. Chen, L. Wu, X. Chen, and B. Jiang, Multi-solute solid solution behaviour and its effect on the properties of magnesium alloys, *J. Magnes. Alloy.*, 10 (2022) 1786-1820. <https://doi.org/10.1016/j.jma.2022.06.015>

[47] H. Zhang, Y. Zhao, J. Liu, J. Xu, D. Guo, C. Li, Impact of rare earth elements on micro-galvanic corrosion in magnesium alloys: A comparative study of Mg-Nd and Mg-Y binary alloys, *Int. J. Electrochem. Sci.*, 18 (2023) 100160. <https://doi.org/10.1016/j.ijoes.2023.100160>

[48] R. K. Abd, A. K. Hussein, L. K. Abbas, Synthesis and Characterisation of NiP-TiC-SiC Nanocomposite Coating via Electroless Process on Alumina Substrate, *Eng. Technol. J.*, 41 (2023) 1456-1464. <http://doi.org/10.30684/etj.2023.139852.1444>

[49] S. R. Areef, Effect of (Zn & Mg) on Corrosion Behaviour of Shape Memory Alloys, *Eng. Technol. J.*, 28 (2010) 5651-5659. <https://doi.org/10.30684/etj.28.18.3>

[50] J. Liu, Z. Lv, Z. Wu, J. Zhang, C. Zheng, C. Chen, Research progress on the influence of alloying elements on the corrosion resistance of high-entropy alloys, *J. Alloys Compd.*, 1002 (2024) 175394. <https://doi.org/10.1016/j.jallcom.2024.175394>

[51] H. Liao, M. Wu, D. Deng, W. Zhong, and B. Xiong, Effects of Ti content on the microstructure, mechanical properties and corrosion behaviour of Ti_xZrNb alloys, *J. Mater. Res. Technol.*, 19 (2022) 1433-1443. <https://doi.org/10.1016/j.jmrt.2022.05.140>